A Global Analysis of the Receptor Tyrosine Kinase–Protein Phosphatase Interactome

Article *in* Molecular cell · January 2017

DOI: 10.1016/j.molcel.2016.12.004

19 authors, including:

Zhong Yao
University of Toronto

Victoria Wong
University of Toronto

Mohan Babu
University of Toronto

Anne-Claude Gingras
Mount Sinai Hospital, Toronto

Resource

Molecular Cell

A Global Analysis of the Receptor Tyrosine Kinase-Protein Phosphatase Interactome

Graphical Abstract

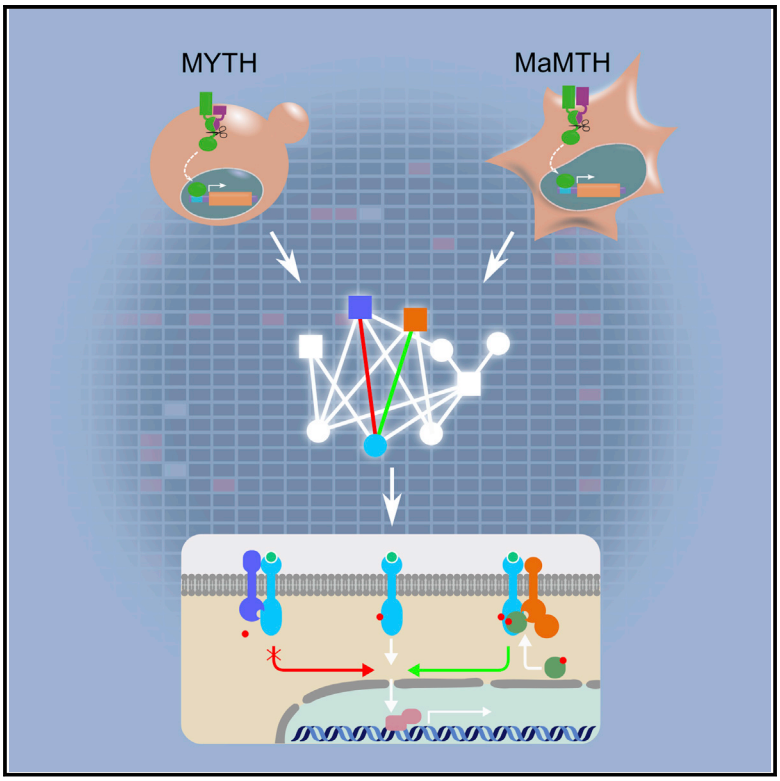

Authors

Zhong Yao, Katelyn Darowski, Nicole St-Denis, ..., Mohan Babu, Anne-Claude Gingras, Igor Stagljar

Correspondence

igor.stagljar@utoronto.ca

In Brief

Using MYTH and MaMTH protein interaction assays, Yao et al. performed comprehensive RTK-phosphatase screens and identified diverse interactions. Among many of these, they show that PTPRH and PTPRB inhibit EGFR signaling by directly dephosphorylating EGFR. By contrast, PTPRA potentiates EGFR signaling through activatory dephosphorylation of SRC and facilitating EGFR/SRC association.

Highlights

- MYTH and MaMTH screens identified numerous RTK-phosphatase interactions
- Diversity of RTK/PTP interaction suggests different modes of their functions
- PTPRH and PTPRB inhibit EGFR signaling through direct dephosphorylation
- PTPRA specifically potentiates EGFR interaction through activating SRC

Yao et al., 2017, Molecular Cell *65*, 1–14
January 19, 2017
http://dx.doi.org/10.1016/j.molcel.2016.12.004

CellPress

Please cite this article in press as: Yao et al., A Global Analysis of the Receptor Tyrosine Kinase-Protein Phosphatase Interactome, Molecular Cell (2016), http://dx.doi.org/10.1016/j.molcel.2016.12.004

Molecular Cell
Resource

A Global Analysis of the Receptor Tyrosine Kinase-Protein Phosphatase Interactome

Zhong Yao,[1] Katelyn Darowski,[1] Nicole St-Denis,[2] Victoria Wong,[1] Fabian Offensperger,[1] Annabel Villedieu,[1] Shahreen Amin,[3] Ramy Malty,[3] Hiroyuki Aoki,[3] Hongbo Guo,[1] Yang Xu,[4] Caterina Iorio,[4] Max Kotlyar,[4] Andrew Emili,[1,5] Igor Jurisica,[4,6,7,8] Benjamin G. Neel,[4,6,9,10] Mohan Babu,[3] Anne-Claude Gingras,[2,5] and Igor Stagljar[1,5,9,11,*]
[1]Donnelly Centre, University of Toronto, Toronto, ON M5S 3E1, Canada
[2]Lunenfeld-Tanenbaum Research Institute at Mount Sinai, Toronto, ON M5G 1X5, Canada
[3]Department of Biochemistry, University of Regina, Regina, SK S4S 0A2, Canada
[4]Princess Margaret Cancer Centre, University Health Network, Toronto, ON M5G 1L7, Canada
[5]Department of Molecular Genetics, University of Toronto, Toronto, ON M5S 1A8, Canada
[6]Department of Medical Biophysics, University of Toronto, Toronto, ON M5G 1L7, Canada
[7]Department of Computer Science, University of Toronto, Toronto, ON M5S 3G4, Canada
[8]Institute of Neuroimmunology, Slovak Academy of Sciences, 845 10 Bratislava, Slovak Republic
[9]Department of Biochemistry, University of Toronto, Toronto, ON M5S 1A8, Canada
[10]Present address: Laura and Isaac Perlmutter Cancer Center, NYU-Langone Medical Center, New York, NY 10016, USA
[11]Lead Contact
*Correspondence: igor.stagljar@utoronto.ca
http://dx.doi.org/10.1016/j.molcel.2016.12.004

SUMMARY

Receptor tyrosine kinases (RTKs) and protein phosphatases comprise protein families that play crucial roles in cell signaling. We used two protein-protein interaction (PPI) approaches, the membrane yeast two-hybrid (MYTH) and the mammalian membrane two-hybrid (MaMTH), to map the PPIs between human RTKs and phosphatases. The resulting RTK-phosphatase interactome reveals a considerable number of previously unidentified interactions and suggests specific roles for different phosphatase families. Additionally, the differential PPIs of some protein tyrosine phosphatases (PTPs) and their mutants suggest diverse mechanisms of these PTPs in the regulation of RTK signaling. We further found that PTPRH and PTPRB directly dephosphorylate EGFR and repress its downstream signaling. By contrast, PTPRA plays a dual role in EGFR signaling: besides facilitating EGFR dephosphorylation, it enhances downstream ERK signaling by activating SRC. This comprehensive RTK-phosphatase interactome study provides a broad and deep view of RTK signaling.

INTRODUCTION

Receptor tyrosine kinases (RTKs) receive varied extracellular chemical signals and process and relay the information to the intracellular space (Lemmon and Schlessinger, 2010). Consequently, RTKs play essential roles in the regulation of multiple cellular processes. Aberrant regulation of these signaling processes can cause various disorders. Therefore, delineating the detailed molecular mechanisms of RTK signaling is critical to both completely understanding the pathophysiology of many diseases and the development of new preventative and treatment measures.

The human genome harbors 58 RTKs (Manning et al., 2002). Their activation leads to tyrosine phosphorylation. The phosphorylated tyrosines recruit downstream proteins that contain SRC homology 2 (SH2) or phosphotyrosine-binding (PTB) domains, which can be enzymes, regulatory proteins, and adaptor proteins that are responsible for activation of multiple downstream cascades. Some recruited proteins are also involved in negative regulation of RTK signaling. RTKs also undergo Ser/Thr phosphorylation although the function of most Ser/Thr phosphorylation is still not fully understood.

Dephosphorylation of RTKs is carried out by protein phosphatases. Approximately 140 protein phosphatases (if one counts only catalytic subunits for multi-subunit phosphatases) have been identified in the human genome. Unlike kinases, protein phosphatases evolved from distinct genes and employ different enzymatic mechanisms (Li et al., 2013). They are traditionally divided into two classes, protein Ser/Thr phosphatases (PSPs) and protein tyrosine phosphatases (PTPs). PSPs include the PPP, PPM, and FCP/SCP families (Li et al., 2013). The cysteine-based PTP superfamily includes about 100 members (Alonso et al., 2004; Tonks, 2006) grouped into classical PTPs and dual specificity phosphatases (DUSPs). Classical PTPs play critical roles in tyrosine kinase signaling (Neel and Tonks, 1997), whereas DUSPs can dephosphorylate Tyr and Ser/Thr residues. Some DUSPs function as lipid or glycogen phosphatases. The EYA family comprises a small set with an aspartate-based catalytic domain (Alonso et al., 2004; Jemc and Rebay, 2007).

As RTK signaling is reversible, the removal of phosphate is as important as its addition. However, the role of phosphatases is less appreciated than that of kinases, and they have long been considered simply and erroneously as signal erasers. Such an over-simplified model ignores the complexities and precision

of RTK signaling. To fully understand the complex picture of RTK signaling, comprehensive studies of phosphatase involvement are needed. We sought to address this question at a systems level from the perspective of RTK-phosphatase protein-protein interactions (PPIs). We previously developed the membrane yeast two-hybrid (MYTH) system (Mak et al., 2012; Snider et al., 2013, 2010; Stagljar et al., 1998; Thaminy et al., 2003) and its mammalian version, mammalian membrane two-hybrid (MaMTH) system (Petschnigg et al., 2014), to study membrane PPIs. In this study, we used both systems to map the genome-wide RTK-phosphatase interactome. Our comprehensive screens identified a large number of PPIs, most of which have not been reported previously, suggesting distinct roles of individual phosphatases in RTK signaling. Furthermore, we revealed molecular details on how PTPRH, PTPRB, and PTPRA help regulate epidermal growth factor receptor (EGFR) signaling.

RESULTS

MYTH Genome-wide Screens Identified Numerous RTK-phosphatase Interactions

We undertook a systematic identification of RTK-phosphatase interactions using the MYTH assay (Figure 1A). We collected cDNAs for 57 of the 58 mammalian RTKs (Manning et al., 2002), the exception being EPHA10. These included 55 human RTKs and two mouse RTKs (MST1R and EPHA5), for which the human cDNAs were not available. RTK cDNAs were cloned into a bait vector plasmid encoding Cub-LexA-VP16 at the 3′ end of the bait open reading frame (ORF). RTK signal peptide sequences were replaced by the mating factor α signal sequence (Figure S1A) to ensure correct sorting in yeast cells (Deribe et al., 2009). Expression and correct membrane insertion of baits were validated by the NubG/I test (Deribe et al., 2009; Usenovic et al., 2012). Six baits (FLT1, FLT3, DDR1, DDR2, AXL, and MERTK) did not pass the NubG/I test and were excluded from the screening. We also examined bait expression by western blot analysis with α-VP16 antibodies recognizing a portion of the artificial transcription factor consisting of LexA-VP16 moiety (Figure S1B, top panel). Expression of LMTK3, FGFR1, and ROS RTKs was not observed, and they were also excluded from the screen. For the rest (48/58 RTKs), the apparent molecular weight of the protein band with the slowest mobility was similar to, or higher than, the calculated value, consistent with expression of the full-length RTK. Additional lower molecular weight bands for many baits could represent the cleavage due to their heterologous expression in yeast. Because the anti-VP16 antibodies recognize the C terminus of each protein and the apparent molecular weight was similar to or higher than the sum of the transmembrane region and the intracellular part of each bait protein, we reasoned that the cleavage sites must be within the extracellular region, leaving the intracellular parts intact.

We also determined the activity state of the expressed RTKs using an α-phosphotyrosine antibody (Figure S1B, lower panel). In total, at least 20 RTKs were constitutively active at significant levels in yeast cells, possibly a result of overexpression or clustering of RTK molecules. Extensive cellular tyrosine phosphorylation was observed in several bait samples, suggesting that these RTKs were highly activated and therefore phosphorylated endogenous yeast proteins in addition to themselves. To functionally characterize RTK phosphorylation, we performed a MYTH assay using active EGFR (L858R mutant) or ERBB2 as bait and SHC1 as prey, a downstream molecule that only binds to activated RTKs. As expected, only the active EGFR and ERBB2 (wild-type [WT]) could interact with SHC1 (Figure S1C). This observation suggests, at least to a certain extent, that RTK phosphorylation in yeast cells mimics that in mammalian cells.

For the MYTH prey library, we collected 141 phosphatase cDNAs, covering all protein phosphatase families (St-Denis et al., 2016). Most of the phosphatases are cytosolic proteins and were cloned into a prey vector encoding an N-terminal Nub tag. A group of PTPs (receptor-type PTPs or RPTPs), of which there were 18 in our collection, are type I transmembrane proteins and were fused to a C-terminal Nub. However, the C-tagged MYTH prey constructs usually had very low signal, a frequent occurrence with tag in this orientation (Snider et al., 2010). Therefore, to avoid false negatives, we decided to study this group separately using MaMTH assay (see below). Fifteen preys (PPP5C, SSU72, UBLCP1, PTPN1, PTPN2, PTPN5, PTPN9, DUSP3, DUSP12, DUSP13B, DUSP22, DUSP23, PTP4A1, PTP4A2, and ACP1) appeared to interact non-specifically, associating with a very high number of RTK baits as well as the unrelated yeast ABC transporter bait BPT1. These were classified as "frequent flyers" and were excluded from the final RTK-phosphatase interactome.

In total, we screened 48 RTK baits against 108 phosphatase preys (Figure 1B; examples shown in Figure S1D) and identified 310 unique PPIs, most of which have not been reported previously. RTK baits differed substantially in their number of interactions, ranging from 0 to 38 (Figure 1C). Several interesting features were observed. The ERBB family of RTKs showed high numbers of PPIs (ranging from 9 to 29), suggesting that they are highly regulated by phosphatases, or vice versa. The lemur tyrosine kinase group members AATK and LMTK2 (LMTK3 was not included due to its poor expression in yeast), whose functions are largely unknown, also interact frequently with phosphatases. Intriguingly, IGF1R and INSR, two RTKs with strong similarity but with distinct biological functions (Siddle, 2012), displayed considerably different phosphatase interactions. Whether this difference helps to determine their signaling specificities merits further exploration. More interestingly, four (PTK7, ERBB3, ROR2, and ROR1) out of eight pseudokinases (EPHA10 was not included in our screen) showed high rates of phosphatase interactions, suggesting the potential regulatory association between phosphatases and these inactive RTKs.

There was also variability in the number of RTK interaction partners for each phosphatase, ranging from 0 to 20 (Figure 1D). Except for the one-member low molecular weight phosphatase family (ACP1 behaves as a frequent flyer), all groups tested contain some members that interact with RTKs. Some groups, such as the PPMs and DUSPs, engaged in a large number of interactions.

Different Types of RTK-PTP Interactions Revealed by Inactive PTP Mutants

The MYTH screen identified many non-receptor-type PTP interactors. Because tyrosine phosphorylation is a central step in

Please cite this article in press as: Yao et al., A Global Analysis of the Receptor Tyrosine Kinase-Protein Phosphatase Interactome, Molecular Cell (2016), http://dx.doi.org/10.1016/j.molcel.2016.12.004

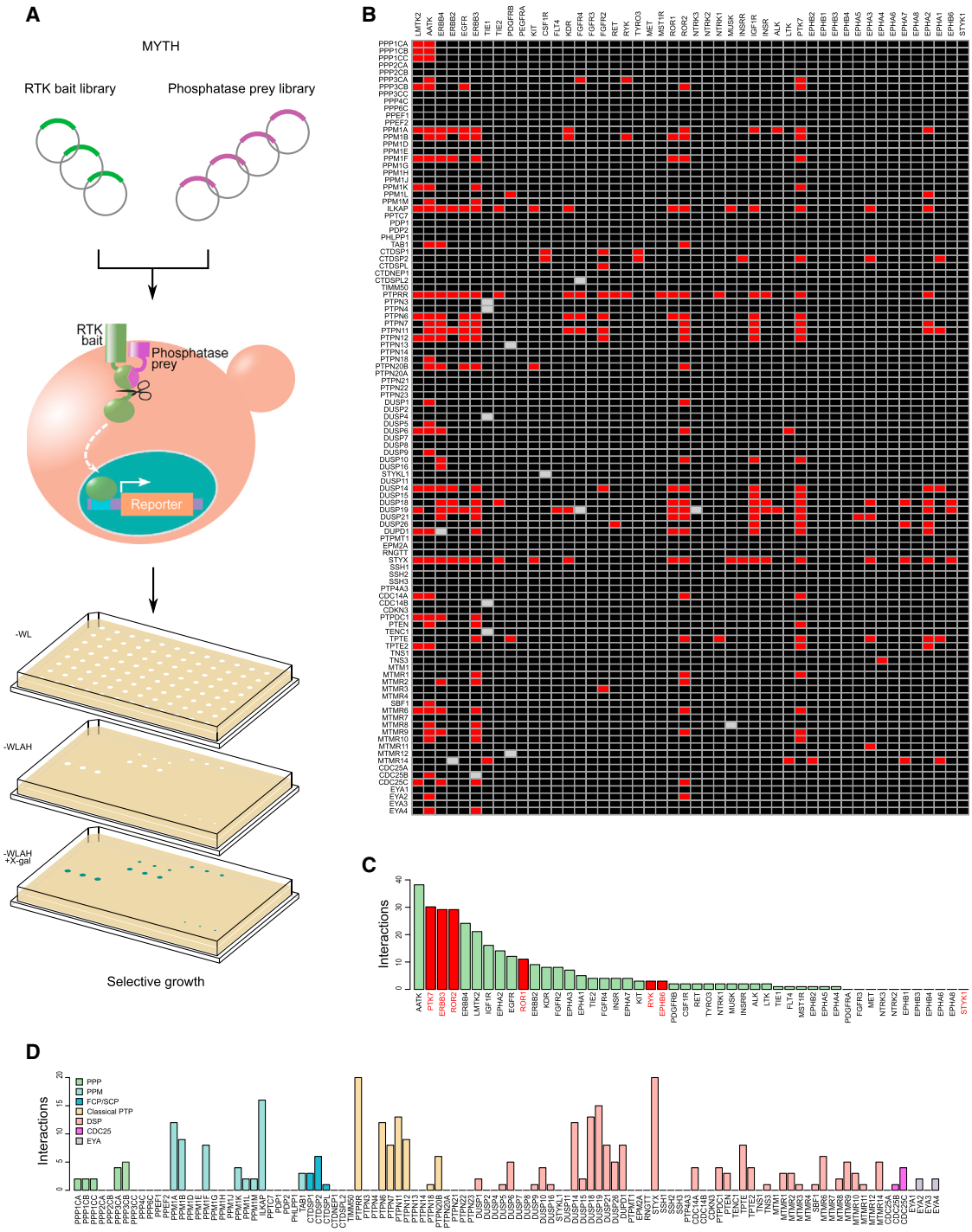

Figure 1. RTK-phosphatase Interactome, as Revealed by MYTH

(A) Scheme for RTK-phosphatase interactome studies using MYTH. RTK baits and phosphatases were co-transformed individually into yeast cells. Interactions were measured as growth on selective medium (SD-WLAH) or the same medium supplemented with X-gal.

(B) RTK-phosphatase interactions are presented as a heatmap. Red rectangles stand for positive interactions and black rectangles indicate no interaction. Failure of the assay for a given pair is shown in gray.

(C) Number of MYTH interactions for each RTK bait. Pseudokinases are indicated in red.

(D) Number of interactions for each phosphatase categorized into family groups indicated by color.

See also Figure S1.

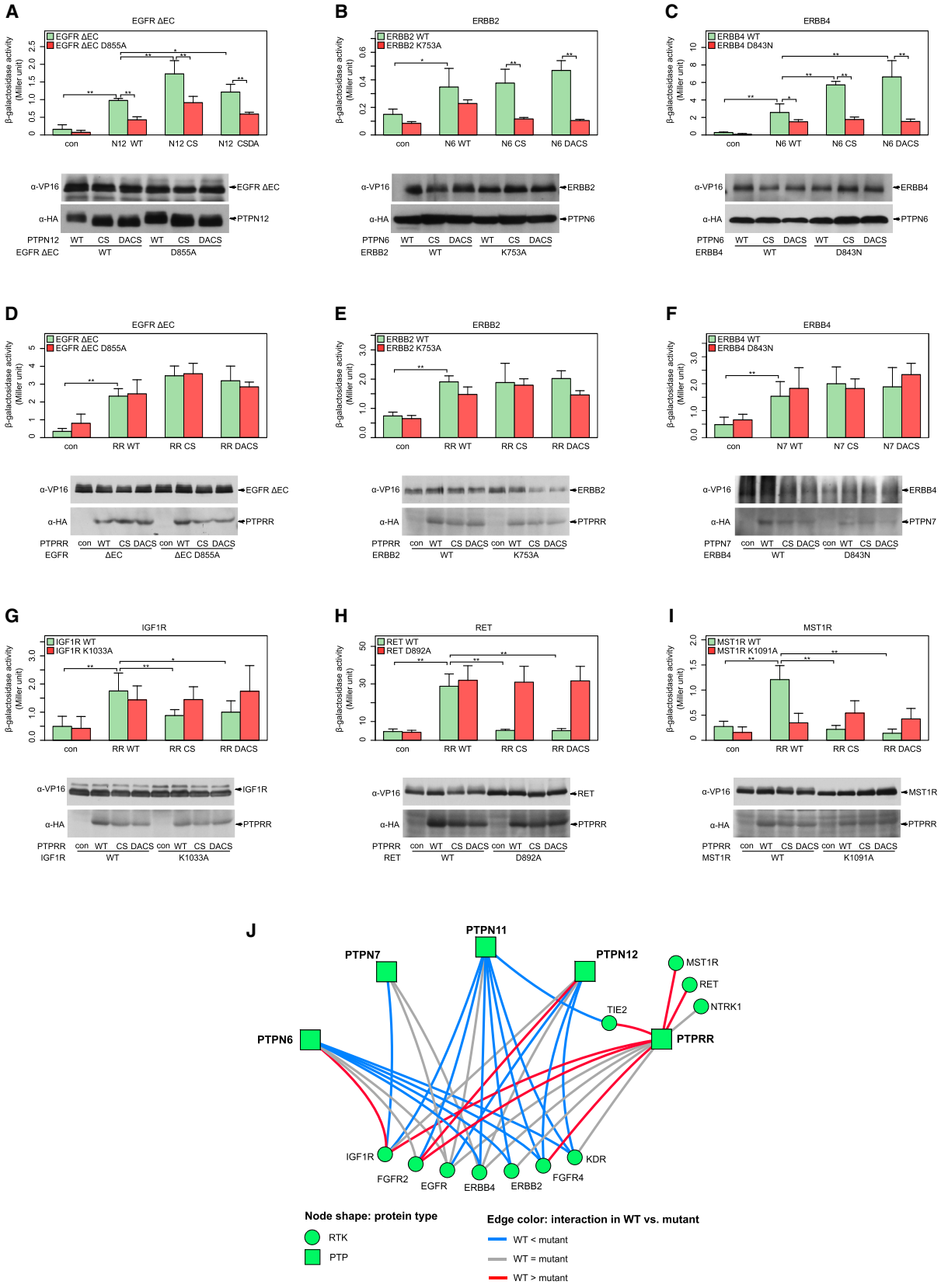

(legend on next page)

RTK signaling, we decided to further characterize this group. PTP "substrate trapping mutants," powerful tools to characterize PTPs and identify PTP substrates (Flint et al., 1997), were used for this purpose. Such mutants are based on the mutations of the key catalytic residue cysteine (C215 in PTPN1) and/or the WPD loop aspartate (D181 in PTPN1) that abolish enzymatic activity but do not abrogate association with its substrates. Two types of PTP trapping mutants were generated for each PTP in our study, the Cys→Ser mutant (CS) and the combined Asp→Ala and Cys→Ser mutant (DACS). A prerequisite for trapping mutant analysis is the presence of tyrosine phosphorylated substrate. As shown above, some RTKs undergo spontaneous activation and thus are phosphorylated constitutively in the yeast cells (Figure S1B). For RTKs that are not active in yeast, activation can be achieved by introducing an activating mutation. For example, EGFR can be activated by deleting the extracellular region (ΔEC) (Endres et al., 2013) (Figure S2A). In total, 13 active RTKs, including EGFR ΔEC, were tested by MYTH assay exemplified in Figure 2 and Figure S2B, among which FLT4 and PDGFRA did not show any interactions. The remaining RTKs showed PPIs of varying strength toward WT and/or mutant PTPs, as assessed by growing serially diluted yeast cells on selective medium (Figure S2B) or, more quantitatively, by performing β-galactosidase assays using ortho-nitrophenyl-β-galactoside (ONPG) as a substrate (Figures 2A–2I).

Three types of PPIs were identified (Figure 2J). In the first type (Figures 2A–2C), the inactive PTP mutants displayed the standard behavior of a trapping mutant, with at least one of the CS or DACS mutants showing enhanced interaction with the RTK compared with the cognate WT PTP (WT < mutant). Inactivating the RTK by mutation markedly attenuated or fully abolished these enhanced PPIs, indicating that autophosphorylation of a particular RTK mediates the PPI. These results strongly suggest that these RTKs are substrates of the interacting PTP. To corroborate this, we performed an in vitro phosphatase assay on selected PPIs: ERBB2/PTPN6, ERBB2/PTPN11, ERBB4/PTPN6, and ERBB4/PTPN11. Phosphorylated ERBB2 and ERBB4 were incubated with recombinant PTPN6 or PTPN11 proteins, and their dephosphorylation was monitored by general anti-phosphotyrosine antibody (Figure S3A), verifying a potential enzyme-substrate relationship. Blotting with α-ERBB4 pY984 antibody suggests that this position is a specific substrate site for PTPN6 and PTPN11. Although the anti-ERBB2 pY1221/1222 antibody did not detect any change in PTP-treated samples, indicating that these two sites are not subject to PTPN6 or PTPN11 regulation, the general anti-phosphotyrosine antibody detected dephosphorylation of ERBB2 by both PTPN6 and PTPN11.

In the second type of RTK-phosphatase PPIs (Figures 2D–2F), no significant difference was observed between WT and mutant PTPs (WT = mutant). These findings were accompanied by the fact that inactivation of the RTK did not change the interaction, suggesting that these PTPs interact constitutively with the RTKs.

In the third type (Figures 2G–2I), inactivating PTP mutations surprisingly attenuated the interaction with active RTK (WT > mutant). As the attenuation was highly dependent on the kinase activity of the involved RTK (as shown by the fact that inactivating the RTK either partially or fully restored the interaction), we hypothesized that the RTK phosphorylates the associated PTP, and phosphorylation releases the PTP. We tested this hypothesis using PTPRR (the isoform we used is an alternatively spliced form that lacks its extracellular region and the transmembrane domain; Shiozuka et al., 1995). PTPRR has been identified as a major MAPK phosphatase (Pulido et al., 1998) but was capable of interacting with many RTKs in our MYTH assay (Figure 1B). Many of its PPIs display a WT > mutant-type interaction. We individually mutated three tyrosines in PTPRR, Y249, Y370, and Y504 (numbered according to the full length isoform α), whose phosphorylation is documented in the database PhosphoSitePlus (http://www.phosphosite.org). Two mutations (of Y370F and Y504F) did not affect its interactions with RET or MST1R (data not shown). Mutation of Y249, however, enhanced the interaction of WT PTPRR toward RET and MST1R, although it had no effect on the PTPRR inactive mutant (DACS) (Figures S3B and S3C). This observation supports our hypothesis that tyrosine phosphorylation on PTPRR attenuates its interactions with some RTKs. Since Y249 is located outside the PTP domain at the N terminus of the PTPRR isoform used in our study, further investigation is required to determine how phosphorylation of this site affects its interactions with RTK substrates. Notably, Y249 is distinct from the kinase interaction motif (KIM), which is responsible for the PTPRR/MAPK interaction and also is negatively regulated by phosphorylation (Blanco-Aparicio et al., 1999). Whether Y249 is also involved in the PTPRR/MAPK interaction awaits further examination. Phosphorylation on additional sites also is likely to be important for PTPRR regulation, given that Y249 mutation alone cannot recover the interaction of inactive PTPRR with RET or MST1R.

Interactions between ERBB Family RTKs and RPTPs as Revealed by MaMTH

Because of the limitations of MYTH in detecting interactions between RTKs and RPTPs, we complemented the above MYTH studies using our recently developed MaMTH assay (Figure 3A) (Petschnigg et al., 2014). To this end, we screened ERBB family RTK baits against 18 RPTP preys (Figure 3B) in human HEK293T reporter cells. Values were normalized to the positive control, EGFR/SHC1 interaction. We chose as positive hits those interactions with signals above an arbitrary cutoff value (0.2); under

Figure 2. PTP-Inactive Mutants Demonstrate Different Interaction Behaviors with RTKs in MYTH

(A–I) Representative RTK-PTP mutant interactions, EGFR ΔEC/PTPN12 (A), ERBB2/PTPN6 (B), ERBB4/PTPN6 (C), EGFR ΔEC/PTPRR (D), ERBB2/PTPRR (E), ERBB4/PTPN7 (F), IGF1R/PTPRR (G), RET/PTPRR (H), and MST1R/PTPRR (I), were quantified by ONPG assay. Each column represents mean ± SD (n = 6). Significance was assessed by one-tailed Student's t test. *$p < 0.05$, **$p < 0.01$. The expression level of each protein was determined by immunoblotting using anti-tag antibodies, VP16 for bait, and HA for prey.

(J) Interaction network between RTKs and PTP-inactive mutants. Interactions are grouped into three categories highlighted in edge color. Blue indicates increased interaction in trapping mutants. Gray represents no obvious difference. Decreased interaction of PTP mutants is represented by red color.

See also Figures S2 and S3.

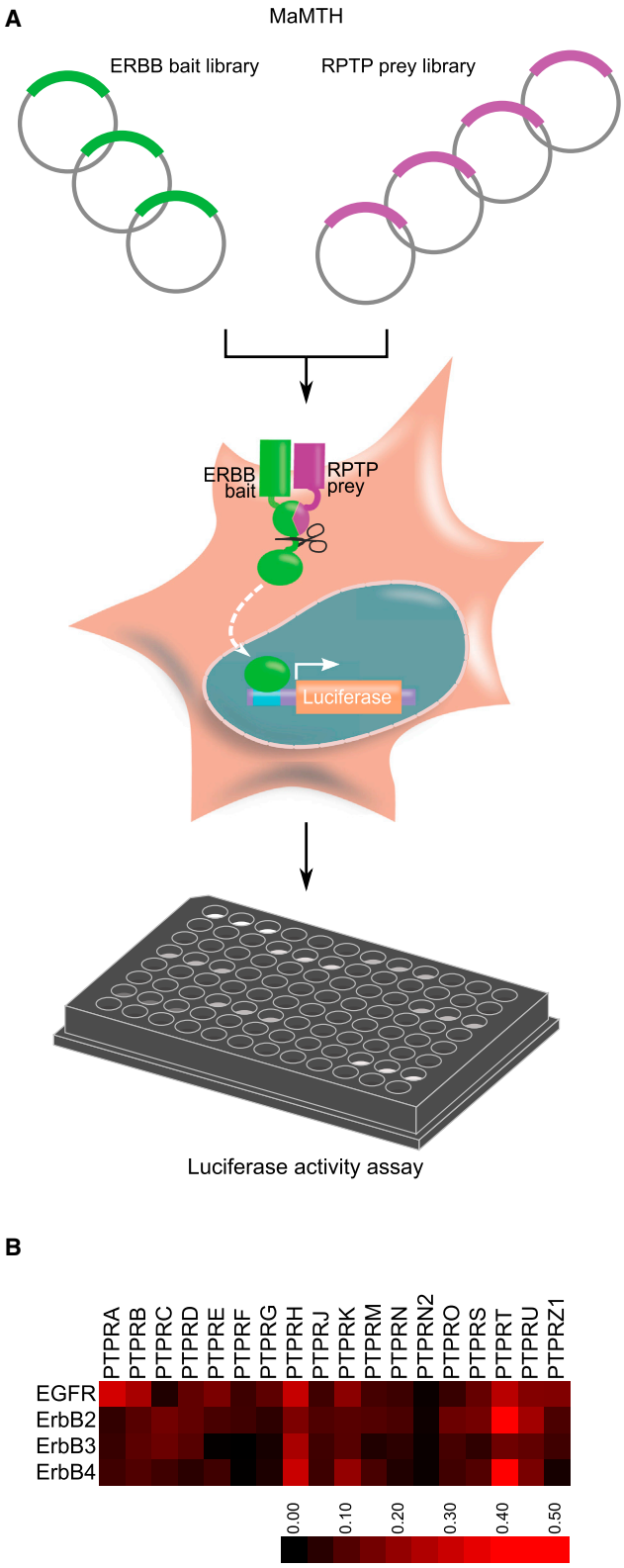

Figure 3. MaMTH Assay Identifies Multiple ERBB-RPTP Interactions
(A) Scheme of MaMTH assay. An ERBB bait was co-transfected with an RPTP prey into reporter cells. Interaction was measured as luciferase activity.
(B) ERBB-RPTP interactions are presented as heatmap. Signals were normalized by the EGFR-SHC1 interaction used as positive control. Each pixel represents the average of triplicate determinations.

these conditions, nine PPIs were identified: EGFR/PTPRA, EGFR/PTPRB, EGFR/PTPRH, EGFR/PTPRT, ERBB2/PTPRT, ERBB2/PTPRU, ERBB3/PTPRH, ERBB4/PTPRH, and ERBB4/PTPRT. The arbitrary criterion of a 0.2 cutoff was set for practical convenience, and hence, we might miss some true PPIs with low signals. Nevertheless, the results showed variation in the ability of ERBB members to interact with specific RPTPs. For example, PTPRH and PTPRT seem to interact with most ERBB family members, whereas PTPRA and PTPRB seem to specifically interact only with EGFR (Figure 3B). Notably, PTPRJ has been previously identified as an EGFR phosphatase and has been shown to interact with EGFR by fluorescence resonance energy transfer (FRET) (Tarcic et al., 2009). The fact that this interaction was not detected by MaMTH might indicate that it is more transient.

Validation of RTK-phosphatase Interactome

The MYTH assay identified 314 RTK-phosphatase PPIs, including four PPIs—ERBB2/PTPN6, TIE2/PTPN11, FGFR4/PTPN12, and KDR/PTPN12—identified only by trapping mutant MYTH assay. MaMTH identified nine additional PPIs. Seventy-four RTK-phosphatase PPIs have been reported previously, according to the Integrated Interaction Database (IID) (Kotlyar et al., 2016), which combines data from major PPI databases. Fifteen of the interactions (20.3%) in this dataset could be reproduced using the MYTH assay (Figure 4A). Therefore, 299 (95.2%) of the MYTH hits have not been reported previously (Figures S4A and S4C). Comparison of their global interactions showed that RTK-phosphatase PPIs occupy a considerable fraction of the global PPIs for some RTKs or phosphatases (Figures S4B and S4D). This outcome might result from the bias of our and previous studies, which mainly focused on RTK-phosphatases interactions.

Of the 74 interactions documented in the PPI databases, 59 (79.7%) were not detected by MYTH (Figure 4A). Failure to detect these interactions might be due to factors such as incorrect folding or mislocalization of the proteins in yeast cells. Another possibility, borne out by detailed comparison of the methods employed for PPI detection, is the bias of MYTH for stable interactions (Figures S4E–S4G). For example, 14 PPIs were previously identified by the conventional yeast two-hybrid assay, of which seven (50.0%) can be reproduced by MYTH (Figure S4E). Of the 36 PPIs identified by affinity-based methods, including affinity chromatography, co-immunoprecipitation (co-IP), pull-down assay, and tandem affinity purification, 12 (33.3%) can be reproduced by MYTH assay (Figure S4F). However, for those identified by activity assay, which captured transient enzyme-substrate interactions, only one out of 16 (6.3%) can be reproduced in MYTH (Figure S4G). Collectively, these results show that the MYTH assay is better at detecting stable PPIs than transient interactions in the case of the RTK-phosphatase protein family.

We further validated a subset of RTK-phosphatase interactions using co-immunoprecipitation. Here, 11 FLAG-tagged phosphatase preys were individually integrated into Flp-In

Please cite this article in press as: Yao et al., A Global Analysis of the Receptor Tyrosine Kinase-Protein Phosphatase Interactome, Molecular Cell (2016), http://dx.doi.org/10.1016/j.molcel.2016.12.004

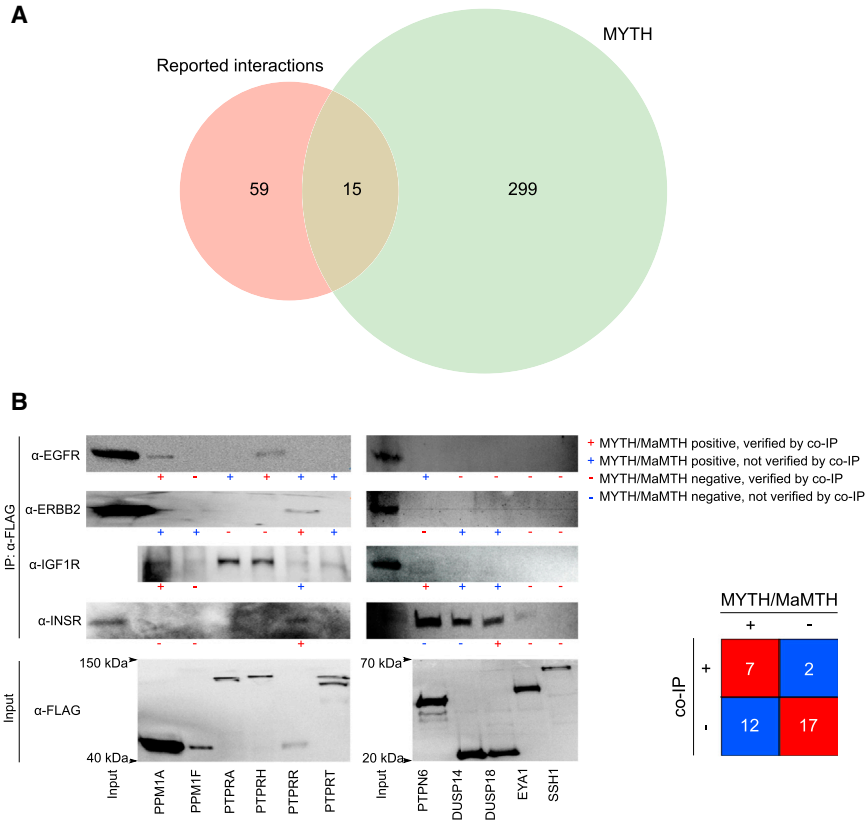

Figure 4. Validation of the RTK-phosphatase Interactome

(A) The RTK-phosphatase interactome revealed by MYTH is compared with previously reported interactions from IID.

(B) Validation of selected RTK-phosphatase interactions by co-IP. Indicated FLAG-tagged phosphatases were integrated into Flp-In T-Rex HEK293 cells and their expression was induced by tetracycline. They were precipitated with α-FLAG antibody, and their interactions with endogenous RTKs were probed by antibodies against indicated RTKs. The MYTH/MaMTH results for each pair are highlighted as + or − beneath each band with red color if validated or blue if not confirmed by co-IP. See also Figure S4.

T-REx HEK293 cells. Their potential interactions with four endogenous RTKs (ERGF, ERBB2, IGF1R, and INSR), including 19 MYTH/MaMTH "positive PPIs" and 19 "negative PPIs," were tested by co-IP with α-FLAG antibody (Figure 4B). Seven (36.8%) MYTH/MaMTH positive PPIs were verified by co-IP. Of the 19 negative PPIs, two (10.5%) were shown to be positive, including INSR-PTPN6 interaction, which is documented in PPI databases but was missed by the MYTH assay. These results provide an assessment of the reliability of the RTK-phosphatase interactions detected by our MYTH and MaMTH assays.

PTPRH and PTPRB Are Direct EGFR Phosphatases that Inhibit EGFR Signaling

The genome-wide RTK-phosphatase interactome revealed in our study contains a wide spectrum of PPIs, most of which have not been reported previously. The biological functions of these interactions are largely unknown; indeed, the overall roles of specific RPTPs in various RTK signaling pathways have not been well elucidated. We sought to address this deficiency and focused on EGFR and its interactions with RPTPs, i.e., PTPRA, PTPRB, and PTPRH, as defined by MaMTH. The subsequent co-IP validation verified the EGFR/PTPRH interaction (Figure 4B) but failed to detect interaction between EGFR and PTPRA. We suspect this was caused by failure of the co-IP to preserve the intactness of the protein complex in the membrane environment under the specific experimental conditions. Thus, we optimized our co-IP condition (see Supplemental Experimental Procedures), although the original one used in Figure 4B works well for general use. The optimized experimental procedure did allow us to detect both EGFR/PTPRA and EGFR/PTPRH interactions (Figure S5A). By contrast, no significant PPIs of ERBB2 with the tested RPTPs were observed, consistent with the MaMTH screen. Although the EGFR/PTPRB interaction identified by MaMTH was not observed in this assay, it was verified by a functional study showing that PTPRB dephosphorylated EGFR as described below (Figure 5B), which may reflect a more transient interaction. We also explored the effect of EGFR kinase activity on EGFR-RPTP interactions by MaMTH assay by using WT or inactive (D885A) EGFR as bait. These results (Figure S5B) demonstrate that EGFR/PTPRA and EGFR/PTPRB PPIs were attenuated by EGFR inactivation, suggesting that these PPIs rely on EGFR activation or phosphorylation. By contrast, the EGFR/PTPRH PPI was not affected, indicating a constant interaction.

We further investigated the functions of PTPRH and PTPRB, which belong to the "R3" subgroup (Andersen et al., 2004), first by overexpressing FLAG-tagged proteins in HEK293 cells (Figures 5A and 5B). Blotting with a general α-pY antibody or a specific α-pY1197 EGFR antibodies showed that their overexpression attenuated tyrosine phosphorylation of EGFR basally or upon epidermal growth factor (EGF) stimulation. This suppression also caused inhibition of the downstream RAS/ERK pathway, suggesting that PTPRH and PTPRB are EGFR phosphatases that can inhibit EGFR signaling (Figures 5A and 5B). The effects of PTPRH were also examined at lower expression levels. To do so, PTPRH was integrated into Flp-In T-REx HEK293 cells, and its expression was induced by treating the cells with varying amounts of tetracycline. The overall trend of EGFR dephosphorylation was consistent with a tetracycline dose-response relationship (Figure 5C).

To further examine the function of PTPRH under physiological conditions, we studied EGFR signaling in the context of *PTPRH* deletion. We used a human ovarian cancer cell line, OV-90, for this purpose, as the expression level of PTPRH in most other commonly used cell lines is low. *PTPRH* knockout was achieved

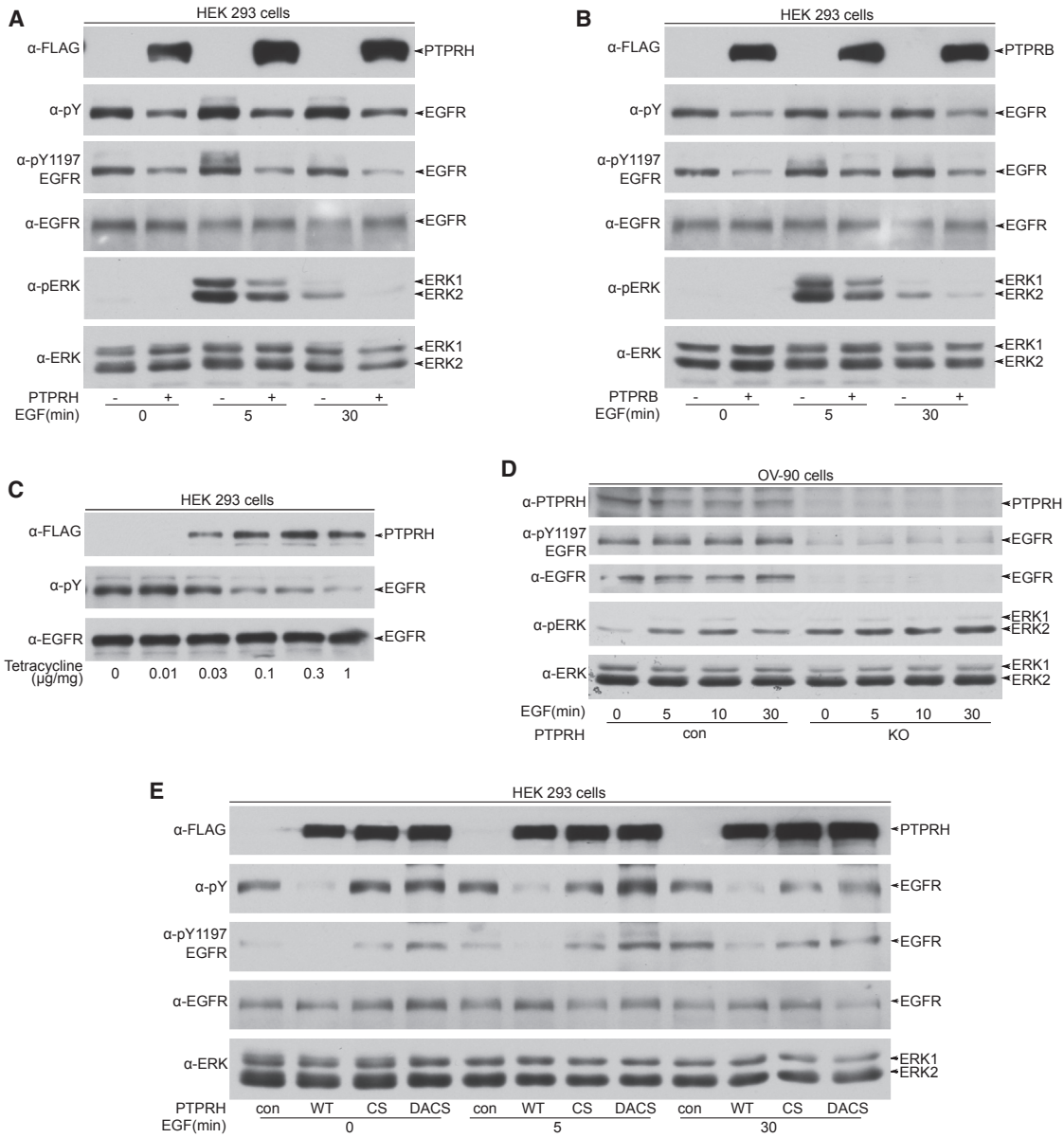

Intensities of phosphopeptides identified by MS

Peptide	Tyr position	Peptide intensity		
		Control	WT	DACS
RPAGSVQNPVY(ph)HNQPLNPAPSR	1110	1036100	*0	126060
GSTAENAEY(ph)LR	1197	635330	*0	870220
LLGAEEKEY(ph)HAEGGKVPIK	869	417410	*0	*75156
GPDNCIQCAHY(ph)IDGPHCVK	585	228290	*0	*41675
GSHQISLDNPDY(ph)QQDFFPK	1172	*0	*0	425391

*: manually validated

Figure 5. PTPRH and PTPRB Are EGFR Inhibitory Phosphatases

(A and B) PTPRH-FLAG (A) or PTPRB-FLAG (B) was transfected into HEK293 cells. The cells were stimulated with EGF followed by western blot analysis.

(C) Dose-response impact of PTPRH on EGFR phosphorylation. PTPRH-FLAG was integrated into FlpIn T-REx HEK293 cells, and its expression was controlled by different concentrations of tetracycline. PTPRH expression and EGFR phosphorylation were measured by western blot analysis.

(legend continued on next page)

using the CRISPR/Cas9 system (Cong et al., 2013; Ran et al., 2013) and was verified by blotting with α-PTPRH antibodies (Figure 5D). PTPRH deficiency markedly increased basal ERK activation (Figure 5D), whereas stimulation with EGF further enhanced and prolonged ERK activation. Interestingly, EGFR levels were reduced significantly in the PTPRH-deleted cells, possibly reflecting downstream negative feedback mechanisms activated by the absence of PTPRH expression. Nevertheless, the residual low levels of EGFR maintained high activity (Figure 5D). These results strongly support that PTPRH is a negative regulator of EGFR signaling. The profound effects of *PTPRH* knockout suggest that the function of PTPRH was not fully compensated by other PTPs and therefore it might be the major PTP for inhibiting EGFR signaling in OV-90 cells.

To understand the molecular details of PTPRH action, we expressed PTPRH CS mutant or combined DACS mutant in HEK293 cells (Figure 5E). The Cys→Ser mutation abolished PTPRH activity against the EGFR. Interestingly, the DACS mutant behaved the opposite way from the WT by enhancing tyrosine phosphorylation of EGFR upon EGF stimulation at 5 min. Thus, the DACS mutant exhibited the typical trapping mutant behavior of a tight interaction with substrates and protecting dephosphorylation from other endogenous PTPs, consistent with identification of PTPRH as a direct phosphatase on EGFR. It should be considered that the trapping-induced increase of tyrosine phosphorylation is distinct from that derived from EGF-stimulated or *PTPRH* deficiency-induced EGFR activation, as its recruitment of downstream signaling molecules is also physically blocked by the trapping PTP. Therefore, the signal propagation is dampened and downstream negative feedback machinery is less active in downregulating EGFR.

Next, we used mass spectrometry (MS) to map the sites on EGFR that were dephosphorylated upon PTPRH expression. For this purpose, EGFR-GFP and PTPRH-FLAG (WT or DACS) were co-transfected into HEK293 cells. After EGF stimulation for 5 min, EGFR was immunoprecipitated with α-GFP antibody and subjected to MS analysis. A fraction of the sample was processed for phosphopeptide enrichment followed by MS analysis (Figure 5F). The non-enriched samples showed a comparable level of EGFR peptide intensities (2.8×10^{10} for control, 1.4×10^{10} for PTPRH WT, and 2.1×10^{10} for PTPRH trapping mutant). The peptides identified in the phosphopeptide-enriched samples are listed in the Table S1, which lists a number of peptides derived from EGFR, including some peptides with Ser/Thr phosphorylation, and five peptides with tyrosine phosphorylation. All of these phosphotyrosines were detected in the PTPRH DACS-transfected sample but absent in the WT PTPRH-transfected sample, suggesting that PTPRH indeed dephosphorylated these sites. Y1197 phosphorylation is more abundant in the DACS sample than in the control sample, consistent with the immunoblotting results using α-pY1197 antibodies (Figure 5E). Interestingly, phosphorylation of Y1172 could not be detected in the control sample. We reasoned that Y1172 is tightly regulated by endogenous PTPs in the control cells but was protected by PTPRH trapping. Some pTyr peptides (pY585, pY869, and pY1110) showed relatively low abundance in the DACS sample compared to the control. This might result from their higher sensitivities to other endogenous PTPs other than PTPRH. However, overall tyrosine phosphorylation appears higher in the DACS sample, as indicated by immunoblotting with α-pY antibody (Figure 5E). Also of interest, in the non-enriched fractions, a number of PTPRH peptides were also detected in the DACS mutant sample (Figure S5C). The only peptide that is relatively abundant in the WT PTPRH sample but absent in the DACS mutant sample was the WPD loop-containing peptide, which contained the mutation Asp→Ala in the DACS mutant and thereby was impossible to detect in the DACS sample. These results suggest that the DACS mutant co-precipitated with EGFR. The fact that the co-precipitation could be preserved after thorough and stringent washing indicated a tight interaction between EGFR and the trapping mutant, which is further evidence of a direct effect of PTPRH on EGFR.

Similar to PTPRH and PTPRB, PTPRT also interacted with EGFR in the MaMTH assay. Nevertheless, overexpression of PTPRT did not have an apparent impact on EGFR phosphorylation or ERK signaling (Figure S5D). We concluded that the EGFR/PTPRT does not regulate EGFR signaling toward ERK activation. Notably, this observation supports the specificity of PTPRH and PTPRB since dephosphorylation cannot always be achieved simply by overexpressing a PTP.

PTPRA Plays Dual Roles in EGFR Signaling

PTPRA displayed strong interaction with EGFR, but not with ERBB2–ERBB4, in our MaMTH assays. Similar to PTPRH and PTPRB, overexpression of PTPRA in HEK293 cells resulted in EGFR dephosphorylation, as demonstrated by immunoblotting with either α-pY antibody or α-pY1197 EGFR antibodies (Figure 6A). Unexpectedly, expression of PTPRA inactive mutants could still inhibit EGF-induced EGFR phosphorylation (Figure S6A), probably suggesting that EGFR dephosphorylation was not carried out directly by the ecto-expressed PTPRA. This could be due to this mutant trapping SRC and blocking SRC-mediated EGFR phosphorylation. Interestingly, however, PTPRA overexpression had a positive effect on downstream RAS-ERK signaling, as α-pERK immunoblots revealed enhanced ERK phosphorylation at 30 min after EGF stimulation. These data suggest that PTPRA might play a dual role in EGFR signaling (Figure 6A).

It was previously demonstrated that PTPRA is an activating SRC phosphatase (Zheng et al., 1992), as it dephosphorylates

(D) PTPRH was deleted in OV-90 cells by CRISPR/Cas9 technology. The WT and PTPRH knockout cells were stimulated with EGF, and the lysates were subject to western blot analysis.

(E) PTPRH CS or DACS mutant was expressed in HEK293 cells, and their effects on EGFR were investigated by western blot analysis.

(F) EGFR-GFP and PTPRH-FLAG (WT or DACS mutant) were co-transfected into HEK293 cells. After stimulation with EGF for 5 min, EGFR was precipitated by α-GFP antibody and subject to MS analysis. The intensities of EGFR phosphopeptides are listed in the right panel. Lysates were also analyzed by western blot analysis (left).

See also Figure S5 and Table S1.

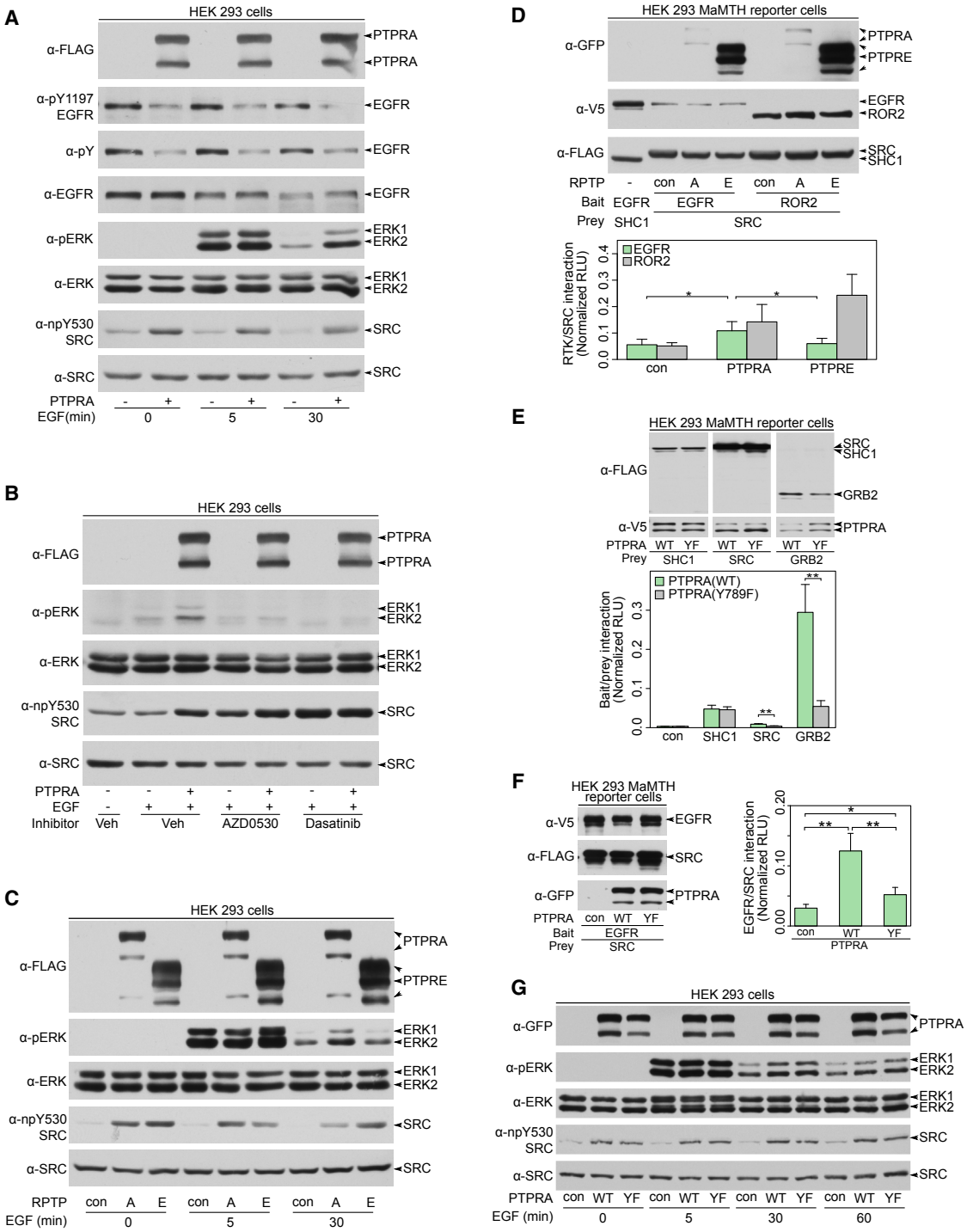

Figure 6. PTPRA Is Involved in EGFR Signaling

(A) HEK293 cells were transfected with PTPRA-FLAG followed by EGF stimulation. Lysates were subject to western blot analysis.

(B) PTPRA-FLAG-transfected HEK293 cells were pretreated with SRC inhibitors, AZD0530, Dasatinib, or vehicle (Veh), for 30 min. After EGF stimulation for 30 min, the cells were subject to western blot analysis.

(C) HEK293 cells transfected with PTPRA-FLAG or PTPRE-FLAG were stimulated with EGF and subject to western blot analysis.

(D) EGFR or ROR2 (control) bait and SRC prey, together with PTPRA-GFP or PTPRE-GFP, were transfected into reporter cells. EGFR-SRC interaction was assessed by MaMTH (lower panel). Signals were normalized by EGFR/SHC1 interaction. Data represent mean ± SD (n = 4). Significance was assessed by one-tailed Student's t test. *$p < 0.05$. The expression of each protein was measured by western blot analysis (upper panel).

(legend continued on next page)

the SRC C-terminal inhibitory phosphorylation site Y530. Immunoblotting with α-non-phosphorylated Y530 antibodies confirmed PTPRA-induced SRC dephosphorylation (Figure 6A). We therefore investigated whether PTPRA-facilitated SRC activation is necessary for PTPRA-induced sustained ERK activation, using two SRC family inhibitors, AZD0530 and Dasatinib. Cells transfected with PTPRA were pre-treated with various inhibitors followed by EGF stimulation for 30 min. As shown in an immunoblot, pre-treatment with SRC inhibitors abolished PTPRA-evoked, late-phase ERK activation (Figure 6B). Therefore, sustained ERK activation in these cells depends on SRC family kinases. In addition, AZD0530 and Dasatinib enhanced SRC Tyr530 dephosphorylation. This might be caused by the inhibitor-induced conformational change of SRC, which leads to uncoupling the interaction between C-terminal SRC kinase (CSK) and SRC (thereby inhibiting Tyr530 phosphorylation by CSK), or by the non-specific effects of the inhibitors on CSK due to the high concentration (1 μM) used in this study.

We next tested whether SRC activation is sufficient to activate the ERK pathway by comparing the effects of PTPRA and PTPRE (Figure 6C). PTPRE is highly similar to PTPRA (Andersen et al., 2004) and is also capable of dephosphorylating SRC on its C-terminal pY (Gil-Henn and Elson, 2003). Notably, our MaMTH assay only showed weak interaction of PTPRE with EGFR (Figure 3B). As expected, both RPTPs dephosphorylated SRC (Figure 6C). However, PTPRE overexpression did not have a significant effect on ERK late-phase activation although it might potentiate ERK activation at 5 min upon EGF stimulation, suggesting that SRC activation is necessary, but not in itself sufficient for PTPRA-induced sustained ERK activation.

Compared with PTPRA, PTPRE only weakly interacts with EGFR in our MaMTH assay (Figure 3) and did not display an effect on EGFR phosphorylation (Figure S6B), prompting us to consider the role of the PTPRA/EGFR interaction in PTPRA-mediated sustained ERK activation. We hypothesized that the binding of PTPRA to EGFR increases the local concentration of competent SRC and facilitates its interaction with EGFR and full activation. This hypothesis was tested with the help of a MaMTH assay in which EGFR (bait) and SRC (prey) were co-transfected into the reporter cells along with PTPRA or PTPRE (Figure 6D). Indeed, there was a significant increase in EGFR/SRC interaction when PTPRA, but not PTPRE or control plasmid, was present. Interestingly, ROR2, which has been shown to interact with SRC (Akbarzadeh et al., 2008; Lai et al., 2012) and was used as a positive control, presented a different pattern: PTPRE exerted a more profound enhancement of the ROR2/SRC interaction than PTPRA. The differential effects of PTPRA and PTPRE suggest a specific role of PTPRA in EGFR signaling and support our model of PTPRA-induced sustained ERK activation (Figure 6E).

We then mapped the region responsible for PTPRA/EGFR interaction by comparing PTPRA and PTPRE molecular elements. Thus, the extracellular region, the transmembrane domain and the intracellular part of PTPRA were replaced with their counterparts in PTPRE, respectively. MaMTH assay using these chimera proteins as preys together with EGFR bait demonstrated that the substitution of the extracellular region of PTPRA exhibited the most marked effect of abolishing PTPRA/EGFR interaction (Figure S6C). Comparison of the sequences of PTPRA and PTPRE reveals that the most significant difference lies in the extracellular regions: PTPRA contains an ~120-amino-acid stretch and PTPRE has a very short (27 residues) extracellular domain. We conclude that PTPRA/EGFR interaction is mainly contributed by the extracellular region of PTPRA. However, the PTPRA intracellular region, as well as its transmembrane domain, may also be involved in the interaction to a certain extent since their substitutions by corresponding PTPRE elements decreased the strength of EGFR/PTPRA interaction (Figure S6C). The observation that inactive EGFR mutation profoundly inhibited EGFR/PTPRA interaction (Figure S5B) also suggests that intracellular interaction is necessary for the full interaction.

It has previously been reported that PTPRA is phosphorylated at Y789 (den Hertog et al., 1994), which plays an essential role in SRC activation by providing a binding site for the SH2 domain of SRC (Zheng et al., 2000). We therefore studied the role of PTPRA Y789 in EGFR signaling and first performed a MaMTH assay using either WT or Y789F PTPRA as bait and SRC as prey (Figure 6E). The Y789F mutation in PTPRA did abolish the PTPRA/SRC interaction, confirming the observation in previous studies. However, the overall interaction strength of WT PTPRA with SRC was low. The exact reason for this is not known but could be that this pY residue also binds GRB2, which competes for PTPRA/SRC interaction. This needs to be clarified in the future. We then tested the effect of the Y789F PTPRA mutant on the EGFR/SRC interaction using a MaMTH assay similar to that in Figure 6D. The results (Figure 6F) clearly show that PTPRA Y789F mutant significantly decreased the EGFR/SRC interaction. Thus, besides regulating direct PTPRA/SRC interaction, Y789 phosphorylation also plays a role in facilitating the EGFR/SRC interactions. However, a subset of EGFR/SRC interaction was not affected by the Y789F mutation, implying the existence of a different pool of SRC able to interact with EGFR in a PTPRA-facilitated, but pY789-independent, manner. Surprisingly, PTPRA Y789F mutation did not affect PTPRA-potentiated ERK activation (Figure 6G). Considering the existence of the pool of PTPRA-facilitated, but pY789-independent, SRC/EGFR interaction as mentioned above, we reason that this pool of SRC may functionally compensate for the loss of pY789-dependent SRC/EGFR interaction. Besides SRC, GRB2 was also reported to

(E) MaMTH assay using PTPRA (WT or Y789F mutant) as bait and PEX13 (negative control), SHC1, SRC, or GRB2 as prey. Data represent mean ± SD (n = 3). Significance was assessed by one-tailed Student's t test. **$p < 0.01$. Expression of each protein is shown in the upper panel.

(F) MaMTH assay with EGFR bait and SRC prey in the presence of WT or Y789F PTPRA mutant. Data represent mean ± SD deviation (n = 3). Significance was assessed by one-tailed Student's t test. *$p < 0.05$; **$p < 0.01$. Protein expression is shown in the left panel.

(G) GFP-tagged PTPRA (WT or Y789F mutant) was transfected into HEK293 cells. After EGF stimulation, the cells were subject to western blot analysis using the indicated antibodies.

See also Figure S6.

interact with pY789 through its SH2 domain (Zheng et al., 2000). Our results in Figure 6E confirm this observation. However, consistent with the previous study, this interaction did not seem to have direct impact on downstream RAS/ERK signaling as displayed in Figure 6G in which no difference in ERK activation was observed between WT and Y789 mutant PTPRA.

DISCUSSION

RTK signaling is a complex process in which phosphorylation and PPIs are two elementary and critical steps. The biophysical features of membrane proteins make it difficult to study the PPIs involved in RTK signaling in their natural membrane environment at the systems level. We used two complementary interaction proteomics approaches, MYTH and MaMTH (Snider et al., 2015; Yao et al., 2015), to characterize the global RTK-phosphatase interactome. As MYTH is performed in yeast, in which mammalian proteins beyond the introduced RTK bait and phosphatase prey are absent, it can largely reduce the complexity and the bias caused by factors such as indirect PPIs, competition, and antagonism of endogenous signaling molecules, as well as the complex behaviors of RTKs in mammalian cells derived from recycling, degradation, and feedback regulation. However, some RTKs are inactive when expressed in yeast, and yeast contains a different spectrum of phosphatases, which together could cause underestimation of phosphorylation-dependent interactions. Phosphorylation-independent interactions should be less biased in a MYTH screen. By contrast, MaMTH works in virtually all mammalian cells and therefore provides a more physiological context for PPI detection between integral membrane proteins.

Our MYTH and MaMTH screens revealed more than 300 RTK-phosphatase interactions, most of which have not been previously reported. All of the phosphatase families tested, although not each member, show some interactions, indicating their potential roles in RTK signaling. However, it should be noted that these interactions are not equivalent to enzyme-substrate interactions and therefore do not necessarily suggest that the involved phosphatase directly dephosphorylates a given RTK or, conversely, that the RTK can phosphorylate the phosphatase. The functions of these interactions can be diverse and need further study.

We paid particular attention to PTPs, as they play critical roles in RTK signaling. Several PTPs showed high levels of interaction with the RTKs in our study. The substrate-trapping behaviors of some mutants support that they are indeed enzymes capable of dephosphorylating the interacting RTKs. However, the "non-trapping" behavior of other PTP inactive mutants suggests different modes of interaction. For example, the PTPs with stable interactions could serve other regulatory functions, such as scaffolding, dephosphorylating other associated proteins, and more. Moreover, several PTP mutants displayed a lower strength of interaction, suggesting a more complex mode of interaction that might involve mutual inhibition.

Although numerous studies have demonstrated that multiple PTPs play inhibitory roles in RTK signaling, several PTPs, such as PTPN11, are also recognized as positive regulators (Neel et al., 2003). Our global RTK-phosphatase interactome provides a basis and guidance for further characterization of the functions of interacting PTPs as exemplified by our in-depth studies. PTPRH and PTPRB are similar RPTPs belonging to subgroup R3 (Andersen et al., 2004) and exhibit similar inhibitory functions toward EGFR in our study. This similarity in function demonstrates the redundancy in the regulation of RTK signaling. Interestingly, another member of the R3 subgroup, PTPRJ, has also been shown to be a strong inhibitory EGFR phosphatase (Tarcic et al., 2009). The fact that PTPRJ/EGFR interaction was not detected in our MaMTH assay might reflect a more transient interaction. Another interesting example is given by the comparison of PTPRA and PTPRE, which are highly similar in sequence and in their capabilities to dephosphorylate and activate SRC (Roskoski, 2005). However, we found that only PTPRA facilitates EGFR downstream signaling. This function correlates with PTPRA's capability of interaction with EGFR, suggesting that this interaction plays an essential role in its regulation of EGFR signaling. This example demonstrates the complexity and specificity of RTK regulation. Additionally, multiple dual-specificity phosphatase hits were detected in our screens. Whether these phosphatases dephosphorylate RTKs or play other roles in RTK signaling awaits future studies.

Serine/threonine phosphorylation also has important effects on RTK signaling. We consistently found numerous PSP hits in our screens, although most of their functions remain unknown. It should be noted that PPPs are typically multi-subunit proteins, composed of a catalytic subunit and scaffold/regulatory subunits that serve to determine their substrate specificities. Since only catalytic subunits were screened, PPP family hits were probably underrepresented by our assay and could be improved by screening scaffolding/regulatory subunits.

In conclusion, through comprehensive investigation of the RTK-phosphatase interactome as well as initial functional studies, we provide a number of new insights into the relationships between RTKs and phosphatases. The RTK-phosphatase interactome reported here represents a rich resource for elucidation of further biological functions of RTKs and phosphatases and might also serve as a guide and a reference for the detailed characterization of individual phosphatases. Furthermore, this study demonstrates the principles of redundancy, specificity, and complexity that govern RTK signaling and broadens our understanding of RTK signaling.

EXPERIMENTAL PROCEDURES

For more methods, please refer to Supplemental Experimental Procedures.

MYTH Assay

MYTH assays were performed as described previously (Snider et al., 2010). The expression and correct subcellular localization were validated by NubG/I test, using plasma membrane protein Fur4 and endoplasmic reticulum (ER) membrane protein Ost1 as preys. Phosphatase prey cDNAs were transformed individually into the bait-containing yeast cells. After colony formation on SD-WL medium, independent colonies were picked and seeded on SD-WLAH or SD-WLAH + X-gal plates in triplicate. Preys with growth on SD-WLAH medium, judged by the formation of significant visually recognized yeast plaques, were considered as positive. Each positive interaction was repeated at least three times. Only those positives that were reproduced in all independent assays

are considered as interactions. Frequent flyers are preys that caused nonselective yeast cell growth on selective media when expressed with most baits. They were predetermined by MYTH using an unrelated protein, yeast integral membrane ABC transporter, BPT1, as the bait. A quantitative ONPG assay was used to compare the interaction strength of different PTP mutants. Here, colonies were picked (six replicates) and grown in SD-WL liquid medium, and the activity of reporter enzyme β-galactosidase was determined using ONPG as substrate, as described previously (Gietz et al., 1997).

MaMTH Assay

MaMTH assays were carried out as described previously (Petschnigg et al., 2014). Briefly, HEK293T reporter cells were seeded on 96-well plates. Bait and prey plasmid DNA were co-transfected into cells by calcium phosphate precipitation. After 40 hr, the cells were broken by Cell Culture Lysis Reagent (Promega), and luciferase activities were measured by chemiluminescence.

SUPPLEMENTAL INFORMATION

Supplemental Information includes Supplemental Experimental Procedures, six figures, one table and can be found with this article online at http://dx.doi.org/10.1016/j.molcel.2016.12.004.

AUTHOR CONTRIBUTIONS

Z.Y., A.-C.G., and I.S. designed the experiments. Z.Y. and I.S. wrote the paper. Z.Y., K.D., V.W., and F.O. performed MYTH assays. Z.Y. and A.V. performed MaMTH screen. Z.Y. performed biochemical analysis of RPTPs with assistance from C.I. N.S.-D. generated the tetracycline-regulated phosphatase cell lines (Flp-In T-REx HEK293) and, together with Beatriz Gonzalez-Badillo (Acknowledgments), assembled a phosphatase ORF library from cDNA and ORF collections and subcloned them in pcDNA5-FLAG vectors. Y.X. generated a PTP mutant cDNA library. S.A., R.M., and H.A. performed co-immunoprecipitation assay. H.G. performed MS analysis. A.E. supervised H.G. M.K. and I.J. performed bioinformatic analysis. A.-C.G. supervised N.S.-D. and B.G.B. B.G.N. supervised Y.X. and C.I. B.G.N., A.-C.G., M.B., I.J., and Laura Riley edited the manuscript.

ACKNOWLEDGMENTS

We thank Laura Riley and Jamie Snider for critical reading of the manuscript, Jason Tjia for technical assistance to MYTH assays, and Beatriz Gonzalez-Badillo for help with assembling the ORF phosphatase collection. Work in the I.S. lab was supported by grants from Ontario Research Fund (GL2-01-018), Canadian Cancer Society Research Institute (CCSRI #702109 and #703889), Canadian Cystic Fibrosis Foundation (CFC #2847), Genome Canada/Ontario Genomics (#9427 and #9428), and Pancreatic Cancer Canada. The I.J. laboratory is supported in part by Ontario Research Fund (GL2-01-030), Natural Sciences Research Council (NSERC #203475), Canada Research Chair Program (CRC #203373 and #225404), Canada Foundation for Innovation (CFI #12301, #203373, #29272, #225404, and #30865), US Army DOD (#W81XWH-12-1-0501), and IBM. Work in the A.-C.G. lab was supported through the Canadian Institutes of Health Research (FDN 143301). A.-C.G. is the Canada Research Chair in Functional Proteomics and the Lea Reichmann Chair in Cancer Proteomics. Work in the M.B. lab was supported through the Canadian Institute of Health Research (MOP12592 and 132191). M.B. is a CIHR New Investigator. Work in the B.G.N. lab was supported by R37 CA49132 and by the Princess Margaret Cancer Foundation. B.G.N. was a Canada Research Chair, Tier I. MaMTH technology is a subject of a PCT patent application (PCT/CA2014/050539) that has been filed by the University of Toronto.

Received: June 8, 2016
Revised: October 13, 2016
Accepted: December 2, 2016
Published: January 5, 2017

REFERENCES

Akbarzadeh, S., Wheldon, L.M., Sweet, S.M.M., Talma, S., Mardakheh, F.K., and Heath, J.K. (2008). The deleted in brachydactyly B domain of ROR2 is required for receptor activation by recruitment of Src. PLoS ONE *3*, e1873.

Alonso, A., Sasin, J., Bottini, N., Friedberg, I., Friedberg, I., Osterman, A., Godzik, A., Hunter, T., Dixon, J., and Mustelin, T. (2004). Protein tyrosine phosphatases in the human genome. Cell *117*, 699–711.

Andersen, J.N., Jansen, P.G., Echwald, S.M., Mortensen, O.H., Fukada, T., Del Vecchio, R., Tonks, N.K., and Møller, N.P.H. (2004). A genomic perspective on protein tyrosine phosphatases: gene structure, pseudogenes, and genetic disease linkage. FASEB J. *18*, 8–30.

Blanco-Aparicio, C., Torres, J., and Pulido, R. (1999). A novel regulatory mechanism of MAP kinases activation and nuclear translocation mediated by PKA and the PTP-SL tyrosine phosphatase. J. Cell Biol. *147*, 1129–1136.

Cong, L., Ran, F.A., Cox, D., Lin, S., Barretto, R., Habib, N., Hsu, P.D., Wu, X., Jiang, W., Marraffini, L.A., and Zhang, F. (2013). Multiplex genome engineering using CRISPR/Cas systems. Science *339*, 819–823.

den Hertog, J., Tracy, S., and Hunter, T. (1994). Phosphorylation of receptor protein-tyrosine phosphatase alpha on Tyr789, a binding site for the SH3-SH2-SH3 adaptor protein GRB-2 in vivo. EMBO J. *13*, 3020–3032.

Deribe, Y.L., Wild, P., Chandrashaker, A., Curak, J., Schmidt, M.H.H., Kalaidzidis, Y., Milutinovic, N., Kratchmarova, I., Buerkle, L., Fetchko, M.J., et al. (2009). Regulation of epidermal growth factor receptor trafficking by lysine deacetylase HDAC6. Sci. Signal. *2*, ra84.

Endres, N.F., Das, R., Smith, A.W., Arkhipov, A., Kovacs, E., Huang, Y., Pelton, J.G., Shan, Y., Shaw, D.E., Wemmer, D.E., et al. (2013). Conformational coupling across the plasma membrane in activation of the EGF receptor. Cell *152*, 543–556.

Flint, A.J., Tiganis, T., Barford, D., and Tonks, N.K. (1997). Development of "substrate-trapping" mutants to identify physiological substrates of protein tyrosine phosphatases. Proc. Natl. Acad. Sci. USA *94*, 1680–1685.

Gietz, R.D., Triggs-Raine, B., Robbins, A., Graham, K.C., and Woods, R.A. (1997). Identification of proteins that interact with a protein of interest: applications of the yeast two-hybrid system. Mol. Cell. Biochem. *172*, 67–79.

Gil-Henn, H., and Elson, A. (2003). Tyrosine phosphatase-epsilon activates Src and supports the transformed phenotype of Neu-induced mammary tumor cells. J. Biol. Chem. *278*, 15579–15586.

Jemc, J., and Rebay, I. (2007). The eyes absent family of phosphotyrosine phosphatases: properties and roles in developmental regulation of transcription. Annu. Rev. Biochem. *76*, 513–538.

Kotlyar, M., Pastrello, C., Sheahan, N., and Jurisica, I. (2016). Integrated interactions database: tissue-specific view of the human and model organism interactomes. Nucleic Acids Res. *44* (D1), D536–D541.

Lai, S.S., Xue, B., Yang, Y., Zhao, L., Chu, C.S., Hao, J.Y., and Wen, C.J. (2012). Ror2-Src signaling in metastasis of mouse melanoma cells is inhibited by NRAGE. Cancer Genet. *205*, 552–562.

Lemmon, M.A., and Schlessinger, J. (2010). Cell signaling by receptor tyrosine kinases. Cell *141*, 1117–1134.

Li, X., Wilmanns, M., Thornton, J., and Köhn, M. (2013). Elucidating human phosphatase-substrate networks. Sci. Signal. *6*, rs10.

Mak, A.B., Nixon, A.M.L., Kittanakom, S., Stewart, J.M., Chen, G.I., Curak, J., Gingras, A.C., Mazitschek, R., Neel, B.G., Stagljar, I., and Moffat, J. (2012). Regulation of CD133 by HDAC6 promotes β-catenin signaling to suppress cancer cell differentiation. Cell Rep. *2*, 951–963.

Manning, G., Whyte, D.B., Martinez, R., Hunter, T., and Sudarsanam, S. (2002). The protein kinase complement of the human genome. Science *298*, 1912–1934.

Neel, B.G., and Tonks, N.K. (1997). Protein tyrosine phosphatases in signal transduction. Curr. Opin. Cell Biol. *9*, 193–204.

Neel, B.G., Gu, H., and Pao, L. (2003). The 'Shp'ing news: SH2 domain-containing tyrosine phosphatases in cell signaling. Trends Biochem. Sci. *28*, 284–293.

Petschnigg, J., Groisman, B., Kotlyar, M., Taipale, M., Zheng, Y., Kurat, C.F., Sayad, A., Sierra, J.R., Mattiazzi Usaj, M., Snider, J., et al. (2014). The mammalian-membrane two-hybrid assay (MaMTH) for probing membrane-protein interactions in human cells. Nat. Methods *11*, 585–592.

Pulido, R., Zúñiga, A., and Ullrich, A. (1998). PTP-SL and STEP protein tyrosine phosphatases regulate the activation of the extracellular signal-regulated kinases ERK1 and ERK2 by association through a kinase interaction motif. EMBO J. *17*, 7337–7350.

Ran, F.A., Hsu, P.D., Wright, J., Agarwala, V., Scott, D.A., and Zhang, F. (2013). Genome engineering using the CRISPR-Cas9 system. Nat. Protoc. *8*, 2281–2308.

Roskoski, R., Jr. (2005). Src kinase regulation by phosphorylation and dephosphorylation. Biochem. Biophys. Res. Commun. *331*, 1–14.

Shiozuka, K., Watanabe, Y., Ikeda, T., Hashimoto, S., and Kawashima, H. (1995). Cloning and expression of PCPTP1 encoding protein tyrosine phosphatase. Gene *162*, 279–284.

Siddle, K. (2012). Molecular basis of signaling specificity of insulin and IGF receptors: neglected corners and recent advances. Front. Endocrinol. (Lausanne) *3*, 34.

Snider, J., Kittanakom, S., Damjanovic, D., Curak, J., Wong, V., and Stagljar, I. (2010). Detecting interactions with membrane proteins using a membrane two-hybrid assay in yeast. Nat. Protoc. *5*, 1281–1293.

Snider, J., Hanif, A., Lee, M.E., Jin, K., Yu, A.R., Graham, C., Chuk, M., Damjanovic, D., Wierzbicka, M., Tang, P., et al. (2013). Mapping the functional yeast ABC transporter interactome. Nat. Chem. Biol. *9*, 565–572.

Snider, J., Kotlyar, M., Saraon, P., Yao, Z., Jurisica, I., and Stagljar, I. (2015). Fundamentals of protein interaction network mapping. Mol. Syst. Biol. *11*, 848.

St-Denis, N., Gupta, G.D., Lin, Z.Y., Gonzalez-Badillo, B., Veri, A.O., Knight, J.D., Rajendran, D., Couzens, A.L., Currie, K.W., Tkach, J.M., et al. (2016). Phenotypic and interaction profiling of the human phosphatases identifies diverse mitotic regulators. Cell Rep. *17*, 2488–2501.

Stagljar, I., Korostensky, C., Johnsson, N., and te Heesen, S. (1998). A genetic system based on split-ubiquitin for the analysis of interactions between membrane proteins in vivo. Proc. Natl. Acad. Sci. USA *95*, 5187–5192.

Tarcic, G., Boguslavsky, S.K., Wakim, J., Kiuchi, T., Liu, A., Reinitz, F., Nathanson, D., Takahashi, T., Mischel, P.S., Ng, T., and Yarden, Y. (2009). An unbiased screen identifies DEP-1 tumor suppressor as a phosphatase controlling EGFR endocytosis. Curr. Biol. *19*, 1788–1798.

Thaminy, S., Auerbach, D., Arnoldo, A., and Stagljar, I. (2003). Identification of novel ErbB3-interacting factors using the split-ubiquitin membrane yeast two-hybrid system. Genome Res. *13*, 1744–1753.

Tonks, N.K. (2006). Protein tyrosine phosphatases: from genes, to function, to disease. Nat. Rev. Mol. Cell Biol. *7*, 833–846.

Usenovic, M., Knight, A.L., Ray, A., Wong, V., Brown, K.R., Caldwell, G.A., Caldwell, K.A., Stagljar, I., and Krainc, D. (2012). Identification of novel ATP13A2 interactors and their role in α-synuclein misfolding and toxicity. Hum. Mol. Genet. *21*, 3785–3794.

Yao, Z., Petschnigg, J., Ketteler, R., and Stagljar, I. (2015). Application guide for omics approaches to cell signaling. Nat. Chem. Biol. *11*, 387–397.

Zheng, X.M., Wang, Y., and Pallen, C.J. (1992). Cell transformation and activation of pp60c-src by overexpression of a protein tyrosine phosphatase. Nature *359*, 336–339.

Zheng, X.M., Resnick, R.J., and Shalloway, D. (2000). A phosphotyrosine displacement mechanism for activation of Src by PTPalpha. EMBO J. *19*, 964–978.